The effect of slow pyrolysis on the conversion of packaging waste plastics (PE and PP) into fuel

Pallab Das, Pankaj Tiwari *

Department of Chemical Engineering, Indian Institute of Technology Guwahati, Guwahati, Assam 781039, India

ABSTRACT

Packaging plastic waste consisting of low and high-density polyethylene and polypropylene were pyrolyzed in a lab scale semi-batch reactor at a very slow dynamic condition (1 °C min^{-1}). Gaseous and liquid products were collected at regular intervals starting from their inception during the degradation process. Detailed analysis was carried out to estimate the properties of plastic derive oil (PDO) obtained at different stages of the pyrolysis process. The pyrolysis temperature has a significant effect on the product compositions. The paraffin concentration increases with increasing pyrolysis temperatures. On the other hand, increased pyrolysis temperature decreases olefin concentration. Olefinic content in the PDO was found comparatively higher when PP was in the feed. Presence of polypropylene in the feed caused the production of PDOs with branch-chain hydrocarbon components with high isoparaffin index and research octane number (RON). The PDOs obtained (for all feed studied) at the early stages of the degradation process have light hydrocarbon liquid fractions belonging to light and middle distillates of petroleum (C_6 – C_{20}). The yield of both light and middle fractions decreased as the pyrolysis reactor temperature reached the maximum value (~400 °C). Gas evolution pattern depends on both pyrolysis temperature and the feed composition. Propylene was found more dominating among other major components of gases like methane, ethane, ethylene, propane, n-butane, 1-butene, isobutylene and n-pentane etc.

© 2018 Elsevier Ltd. All rights reserved.

1. Introduction

Plastics are synthetic organic polymers, which have been serving humans in day-to-day life, because of their large range of physical and chemical attributes like strength, durability, lightweight, flexibility, resistance to the extremity (thermal, electrical and chemical) and their ability to mould into different shapes. The global production of plastics (polymer resins and fibres) in the year 2015 was estimated as 381 million metric tons (MT), increased by 75% since the year 2000 (Geyer et al., 2017). The per capita consumption of plastics in India is around 11 kg/year (2016) whereas average global consumption is about 28 kg/year (Kamyotra and Sinha, 2016). The largest share of plastics consumption is in packaging applications (~44%) (Geyer et al., 2017). The presence of plastic waste in the municipal solid waste (MSW) has been increased from less than 1% in 1960 to more than 10% in recent years (Jambeck et al., 2015). Plastic waste generation leads to huge accumulation, instead of decay in the landfill and in the various natural habitats like rivers and oceans. Thermal treatments like combustion or incineration can eliminate the plastic waste permanently but such processes generate harmful emissions to the environment. Recycling (mechanical/chemical) is a possible path for plastic waste disposal. However, most of the recycling processes are costly, energy intensive and end up producing low-grade products. Pyrolysis is a very viable and sustainable waste management process in the treatment of municipal solid waste containing carbonaceous materials like plastics and biomass (Xue et al., 2016). The process of pyrolysis involves degradation of complex molecules like polymers (plastics) into a short chain, less complex molecules by the application of heat and/or pressure under inert condition. Most plastics pyrolysis plants utilize high temperature (700 °C) to moderate temperature (~500 °C) in the presence of a suitable catalyst (Chattopadhyay et al., 2016; Kaminsky et al., 1995; Kumar et al., 2011; Siddiqui and Redhwi, 2009; Williams and Williams, 1997a, 1999). High-temperature pyrolysis process is generally performed in fluidized bed type reactors for a very short reaction time (fast pyrolysis) which produces excess amount of gaseous products (Kaminsky et al., 1995; Williams and Williams, 1997a). On the other hand, the liquid product obtained under such conditions requires post process up-gradation (distillation) to be utilized as diesel, petrol and fuel oil alternative (Joo and Guin,

* Corresponding author.
  E-mail address: pankaj.tiwari@iitg.ernet.in (P. Tiwari).

1998). Different reactor configurations like batch (Onwudili et al., 2009), semi-batch (Lopez-Urionabarrenechea et al., 2012), fluidized bed (Costa et al., 2010; Kaminsky et al., 2004; Williams and Williams, 1997b, 1999), rotary kiln (Aguado et al., 2002a; Serrano et al., 2003), spouted bed (Aguado et al., 2002b; Elordi et al., 2009), etc. have been utilized for pyrolytic conversion of plastics (individual/mix) into useful products. Microwave-assisted pyrolysis (Ludlow-Palafox and Chase, 2001; Undri et al., 2013) is also gaining attention in the recent times. Various plastic recycling schemes including pyrolysis have been discussed and compared in the recently published review articles (Chaukura et al., 2016; Lopez et al., 2017; Miandad et al., 2016).

To increase the production of high-quality liquid products (fuel), the concept of slow pyrolysis can be applied. The advantage of slow pyrolysis over fast pyrolysis is manifolds, particularly the long duration in slow pyrolysis leads to superior (controlled) heat transfer, better control over flow rates of inlet and outlet (controlled product collection) and high liquid yield. Detailed understanding of slow pyrolysis including the effect of long duration is still lacking in terms of product distribution to target value-added production, and limited reports are available (Marcilla et al., 2009; Onwudili et al., 2009). Onwudili et al. (2009) carried out low-temperature pyrolysis of low-density polyethylene (LDPE) and polystyrene (PS) and their mixture in the range of 350–500 °C for 1 h and 2 h durations. LDPE degradation started at 400 °C and highest yield of oil was reported at 425 °C with a slight alteration in the oil compositions due to the long duration of pyrolysis. Similarly, Wong and Broadbelt (2001) carried out the pyrolysis of polypropylene (PP) and polystyrene (PS) at two isothermal conditions; 350 and 420 °C for two durations, 180 min and 18 h. They observed increase in the conversion with reaction time up to a certain extent (90 min) and further perceived no significant change.

In the current study, three most common plastics comprises of low and high-density polyethylene (LDPE and HDPE) and polypropylene (PP) abundantly used in packaging applications were chosen for slow dynamic (heating rate of 1 °C min^{-1}) pyrolysis studies. The plastic derive oil (PDO) obtained at various intervals during the slow pyrolysis were identified and quantified by various analytical techniques and the gases were analysed and quantified using gas chromatography (GC).

2. Materials

LDPE, HDPE and PP in the form of virgin plastic pellets were acquired from Haldia Petrochemicals, India and waste plastic samples were collected from household plastic waste materials. Virgin plastic pallets (3–5 mm) were manually cut into small grains for thermogravimetric analysis (TGA), whereas for lab scale pyrolysis, the plastic pallets were used directly. Pyrolysis experiments were conducted for three individual plastics (virgin) and their mixture (VMIX) of an equal quantity of each. The samples collected from household materials were segregated for pyrolysis, based on their resin identification code of LDPE, HDPE and PP samples. Cleaned and dried samples were chopped into small pieces of size 1–2 cm and mixed (RMIX) together with an equal quantity of all three

before pyrolysis. The proximate analysis and calorific values of virgin and waste samples (dry) are reported in Table 1.

The liquid hydrocarbon standards (ASTM D5307 internal standards from Supelco) and gas sampling bags (Tedlar bags) were procured from Sigma Aldrich. Gaseous hydrocarbon standard (mixture) and the standard permanent gas mixture (CO_2, CO and H_2) were procured from Chemtron scientific, India and Centurion, India respectively. Dichloromethane (HPLC grade) and Deuterated chloroform ($CdCl_3$ 99.8%) were obtained from Merck (India).

3. Experimental

To assess the degradation range, microscale pyrolysis (TGA) study was carried out for virgin plastic samples (6–10 mg) using NETZSCH 209 F1 TG under the inert atmosphere of N_2 with a flow rate of 60 ml min^{-1} (40 ml min^{-1} as purge and 20 ml min^{-1} as protective gas). The heating rate of 1 °C min^{-1} was maintained in the temperature range of 30–600 °C. The lab-scale pyrolysis experiments were conducted in a semi-batch cylindrical reactor (Supplied by Dass & Co, India) having a capacity of 1000 ml with an internal diameter of 7 cm. The schematic representation of the experimental setup is shown in Fig. 1. A tubular electrical furnace mounted with a PID controller was used as heat source for the pyrolysis. The thermocouple at the outer surface of the reactor was used to maintain the pyrolysis conditions and the temperature at the centre of the rector was recorded. The variations in the reactor temperature with time for the non-isothermal profile is shown in Fig. 1S. Nitrogen (inert) was used as purging gas with a flow rate of 100 ml min^{-1}. Sample amount (W_F) of ~50 g was measured by weighing balance and placed in the reactor core for pyrolysis. The temperature was increased at a rate of 1 °C min^{-1} (slow pyrolysis) to reach a final temperature of 500 °C (furnace temperature) and the final isothermal condition was maintained for 1/2h. Once the minimum degradation temperature was reached, the pyrolysis products started coming out of the reactor and then passed through a long cylindrical water-cooled condenser (<5 °C). The liquid product samples were collected in a cylindrical separating funnel. For each 10 min interval, the liquid product or the plastic derived oil (PDO) was transferred into a 15 ml glass vial for storage and individual analysis. The collection vials were tagged based on the time of its collection from the beginning of the pyrolysis. Similarly, the uncondensed gas stream was collected in tedlar bags (600 ml) at regular intervals and the rest of the time the gas was vented out. The overall yield of gas, liquid and solid products were calculated assuming no mass loss during the pyrolysis process. The amount of liquid (W_l) product was measured by weighing all the individual liquid samples collected. The solid (W_s) amount was calculated from the residue remained in the reactor at the end of the process. The gas yield (W_g) was measured by material balance($W_g = W_F - W_l - W_s$). Each experiment was duplicated and the average values are reported.

Supplementary data associated with this article can be found, in the online version, at https://doi.org/10.1016/j.wasman.2018.08.021.

Table 1
Volatile matter (VM), ash content (AC) fixed carbon (FC) and high heating value (HHV) of the individual samples.

	VM (w/w%)	AC (w/w%)	FC (w/w%)	HHV (MJ/kg)
LDPE (virgin)	99.95	0	0.05	47.12 ± 0.8
HDPE (virgin)	99.97	0	0.03	46.95 ± 0.61
PP (virgin)	99.08	0	0.92	46.67 ± 0.5
LDPE (waste)	79.99	19.25	0.76	44.25 ± 0.35
HDPE (waste)	99.32	0.59	0.09	45.38 ± 0.66
PP (waste)	99.68	0.05	0.27	46.05 ± 0.49

1. Nitrogen cylinder
2. Regulator valve
3. Rotameter
4. Pyrolysis reactor
5. Tubular furnace
6. Thermocouple (TC1, inside the reactor; TC2, outside the reactor for furnace temperature)
7. PID controller
8. Water circulating chiller
9. Condenser
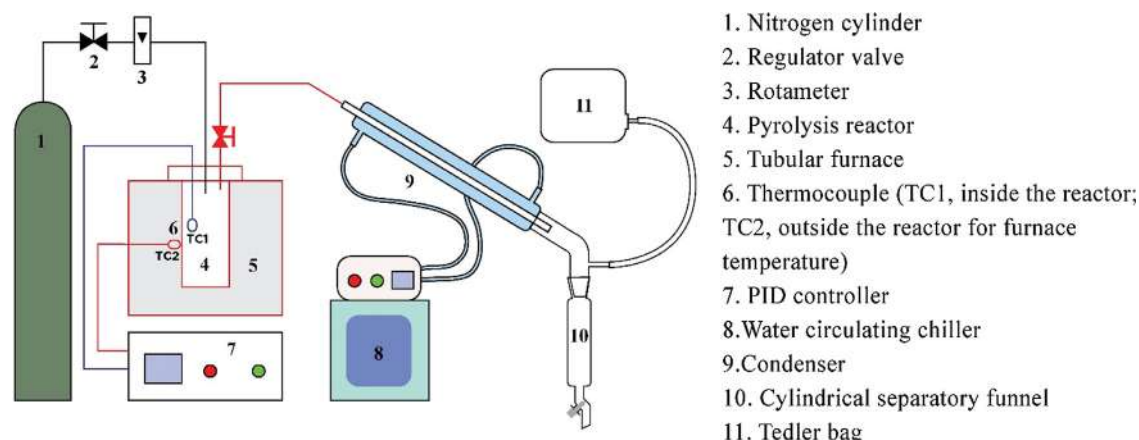10. Cylindrical separatory funnel
11. Tedler bag

Fig. 1. Schematic representation of pyrolysis setup.

3.1. Characterization of plastic derived oil (PDO)

The liquid samples (PDO) were analysed with the help of ^{1}H (proton) nuclear magnetic resonance spectroscopy (NMR), Fourier transform infrared spectroscopy with attenuated total reflection method (FTIR-ATR) in the wave number ranging between 4000 and 600 cm^{-1} and gas chromatography with flame ionization detector (GC-FID).

3.1.1. ^{1}H NMR analysis of PDO

Ascend™ 600 (make: Bruker) spectrometer operating at 600 MHz and 25 °C was used for NMR study. Samples were dissolved in CdCl$_3$ with 0.03 vol% Tetramethylsilane (TMS) as a lock solvent. The chemical shifts were reported as ppm from TMS (lock solvent). The functionality of the compounds present in the PDO sample can be identified from ^{1}H NMR. Using the correlations provided by Myers et al. (1975a,b), the liquid sample can be quantified in terms vol% of paraffin, olefin and aromatic. These correlations were previously applied by Joo and Guin (1998) and Sinag et al. (2006) in the characterisation of similar oil samples. A detailed explanation can be found in our previous study. Additional information like H/C ratio, isoparaffin index and the research octane number (RON) value of the PDOs were determined using these correlations (Eqs. (1)–(6). Table 2 summarizes the spectral region of the parameters (integral area) A, B, C, D, E and F (Fig. 2). These correlations were established based on the known standard mixture (with an error margin of ±2%).

$$Aromatics, vol.\% = \frac{(A+C/3)0.97 \times 10^2}{(A+C/3)0.97+(D-2B+E/2+F/3)1.02+3.33B} \quad (1)$$

$$Paraffins, vol.\% = \frac{(D-2B+E/2+F/3)1.02 \times 10^2}{(A+C/3)0.97+(D-2B+E/2+F/3)1.02+3.33B} \quad (2)$$

$$Olefins, vol.\% = \frac{3.33B \times 10^2}{(A+C/3)0.97+(D-2B+E/2+F/3)1.02+3.33B} \quad (3)$$

$$H/C = \frac{A+B+C+D+E+F}{(A+C/3)1.28+(D-2B+E/2+F/3)1.02+3.42B} \quad (4)$$

A close correlation between the amount of branching in the structure of a paraffinic hydrocarbon and its octane number (Albahri, 2003) leads to the following two properties, *isoparaffin index* and *RON*.

Table 2
NMR spectral region (Myers et al., 1975a,b).

	Proton type	Chemical shift region (ppm)
A	Ring aromatic	6.6–8.0
B	Olefin	4.5–6.0
C	α-methyl	2.0–3.0
D	Methine (paraffins)	1.5–2.0
E	Methylene(paraffins)	1.0–1.5
F	Methyl(paraffins)	0.6–1.0

$$Isoparaffin\ index = CH_3/CH_2 = (F/3)/(E/2) \quad (5)$$

$$RON = 80.2 + 8.9\ isoparaffin\ index + 0.107\ aromatics\ (vol.\%) \quad (6)$$

3.1.2. Simulated distillation (SimDist) analysis of PDO

SimDist analysis is a well-known technique to characterise petroleum fractions for rapid determination of the carbon number distribution (boiling range). The GC (model: GC Trace 1110, make: ThermoFisher scientific) operating conditions for this method is reported in Table 3. Two internal hydrocarbon paraffin standards (ASTM D5307 from Supelco), 48,182 (C$_3$ – C$_9$) and 48,179 (C$_{10}$ – C$_{44}$) were used to determine the retention time of n-paraffins which helped in establishing the carbon number (boiling point) distribution of PDOs. All the liquid samples were filtered with a syringe filter (45 μm) and subsequently diluted with HPLC grade dichloromethane (DCM) up to 1 ppm before analysis.

3.2. Characterisation of non-condensable gases

The non-condensable gases were analysed in the GC using the thermal conductivity detector (TCD) and flame ionisation detector (FID). The GC-TCD was utilized to find out the presence of any permanent gases like CO$_2$, CO and H$_2$ whereas the GC-FID was used to estimate hydrocarbon gas (saturated and unsaturated) concentrations. The GC configuration for TCD and FID analysis has been compiled in Table 3. Gas standards with known concentrations were used to identify and quantify the gaseous components.

4. Results and discussion

4.1. Thermogravimetric analysis and semi-batch pyrolysis yield

To determine the degradation-temperature window of three plastic samples, TGA analysis was carried out at a very slow heating rate (1 °C min^{-1}). Fig. 3 shows TGA and DTG profiles for virgin
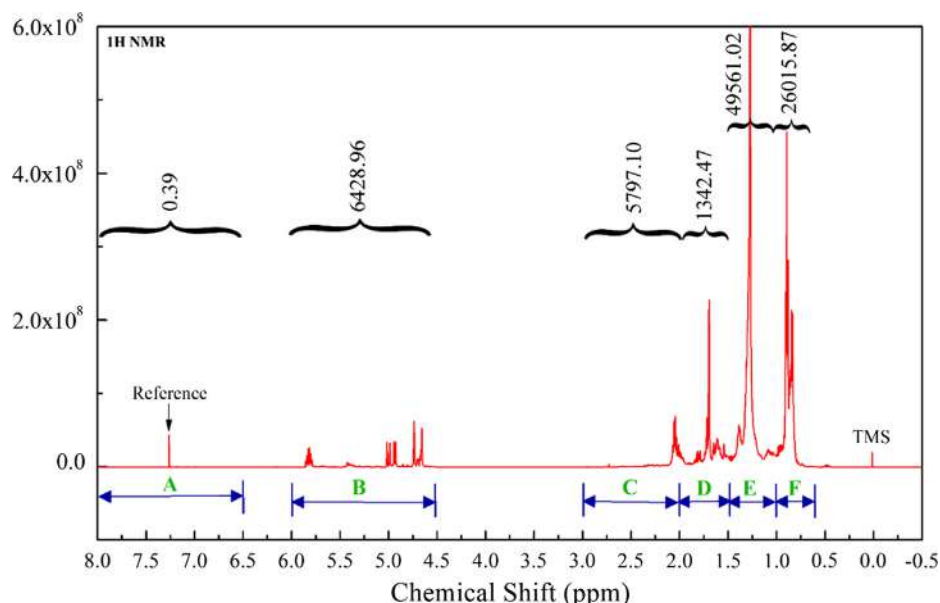
Fig. 2. NMR spectra with different spectral region (A–F) and the integrated area under the curves (for PDO obtained at 400 °C from LDPE).

Table 3
GC configuration for various analysis.

Parameters	GC method		
	GC-Simdist (liquid)	TCD (gas)	FID (Gas)
Column (make)	TR-Simdist (Thermo scientific)	60/80 Carboxen-1000 (Supelco)	TG-BOND Alumina (Thermo scientific)
Length	10 m	4.57 m	30 m
Int. Diameter	0.53 mm	2.1 mm	0.53 mm
Carrier gas	N_2 (high pure)	Helium	Helium
Flow rate (Carrier gas)	8 ml min^{-1}	30 ml min^{-1}	4 ml min^{-1}
Oven temperature program	60 °C (2 min) to 350 °C at 5 °C min^{-1} and 5 min hold	40 °C (5 min) 200 °C at 5 °C min^{-1}	130 °C isothermal (15 min)
Injector temperature	350 °C	150 °C	200 °C
Detector temperature	350 °C	150 °C	200 °C
Sample injection	2 μl	1 ml	1 ml

samples, LDPE, HDPE and PP. Onset temperature (T_o) of LDPE and HDPE were found to be 330 °C and 340 °C respectively, whereas the PP has shown a low onset temperature of 275 °C. Similarly, the peak degradation temperature (T_m) of PP has a lower value

(405 °C) compared to LDPE (430 °C) and HDPE (435 °C). Both onset temperature (T_o) and peak degradation temperature (T_m) values depend on heating rate employed (Das and Tiwari, 2017). Detail explanation of thermal degradation and the TGA based kinetics of plastic samples can be found in our previous study (Das and Tiwari, 2017). It was observed in the DTG plot (Fig. 3) that the rate of weight loss increases with the increase of temperature and pass through a maximum at T_m, then in rest of the process, the rate declines to a minimum value (at the end temperature). Since the rate of degradation is changing with the increase of reaction time (temperature), a change can be expected in the distribution of the product in both the gas and liquid phases. A low onset degradation temperature (T_o) can be achieved by lowering the heating rate. The fact that encouraged to choose a low heating rate of 1 °C min^{-1} in the lab scale pyrolysis of plastics. Small DTG peak appeared at the onset point of LDPE/HDPE, may be due to the impurities (plasticizers/additives) present in the polymer matrix and/or heating rate (low value) effect on degradation mechanism. However, the amount of impurities used in the production of these plastics are relatively low hence, their effect on the pyrolysis product distribution can be neglected. The total yield (%) calculated at the end of each pyrolysis experiment with different feed streams are summarized in Table 4 and the cumulative yield (during PDO production period) with respect to time is shown in Fig. 2S. In case of the mixture of virgin plastic (VMIX), the total PDO yield of
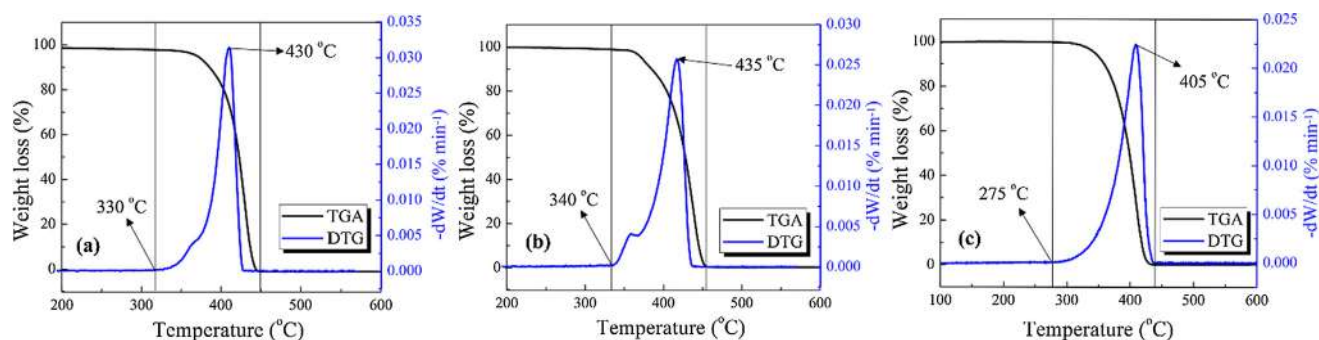

Fig. 3. Non-isothermal (1 °C min^{-1}) TGA and DTG profiles of (a) LDPE, (b) HDPE and (c) PP.

Table 4
Overall product yield (w/w%).

Material	PDO w/w%	Gas w/w%	Residue w/w%
LDPE, virgin (50 g)	82.68	16.88	0.44
HDPE virgin (50 g)	82.66	16.78	0.56
PP virgin (50 g)	83.16	16.53	0.31
VMIX (50 g)	82.25	17.04	0.71
RMIX (50 g)	74.98	21.36	3.66

around 82% was achieved whereas, waste plastic mix (RMIX) could produce 75% yield. A slightly higher yield of liquid (~83%) was obtained in case of PP. The residue obtained for RMIX was quantitatively higher than virgin plastic feed which may be attributed to the impurities (colour, additives etc.) present in the real waste samples.

4.2. Liquid product analysis

4.2.1. FTIR and NMR analyses

FTIR-ATR analysis was carried out for all the PDO samples obtained for all the feed at various time intervals. The spectra obtained are shown in Fig. 4. The identifications of notable peaks for each feed are depicted in Fig. 3S and Table 1S summarizes the functionality of the components. Close examination of the IR signatures implies similar functionality among all the oil samples. Peaks between 2850 and 3000 cm^{-1} represents the characteristics of C – C stretching frequencies. Multiple peaks suggested the presence of methyl and methylene groups. Peaks near 1375 cm^{-1} and 1460 cm^{-1} also confirmed the C – H (sp^3) bending and also the band at 720 cm^{-1} (rocking frequency for adjacent methylene group) approved the presence of long chain paraffinic groups. Peaks appeared at 3075 cm^{-1} denoted the presence of unsaturation (sp^2 C – C stretch), the peak intensity appeared to be slightly higher at the initial PDO samples and when the PP was in the feed. The C = C stretch occured in the region of 1670–1640 cm^{-1}. There was no significant band appeared in the region of 3300 cm^{-1} which

established the absence of any alkyne (sp C – H stretch) group. The FTIR spectra didn't convey any clarity regarding the presence of any aromatics in the PDOs. The complete quantitative estimation of paraffin, olefin and aromatic was carried out by ^{1}H NMR analysis. Total paraffin, olefin and aromatic content of the PDOs obtained at different pyrolysis time and for different feed compositions were determined, using Eqs. (1)–(3) and are reported in Table 5. Initial observations clearly state that the aromaticity of PDOs were very low, although a marginal increase of aromaticity was observed at later stages (higher temperature) of the slow pyrolysis, particularly when the feed was the mixture of real waste (RMIX). Onwudili et al. (2009) reported a decrease of paraffin concentration at high temperature (500 °C) and high pressure (4.31 MPa) pyrolysis followed by the occurrence of cyclization and aromatization reactions which eventually increased the aromatic concentration in the liquid (wax) obtained at higher temperature. The final batch of PDO obtained (at 510 min) for HDPE showed the maximum paraffinic composition (~72 v/v %). On the other hand, the first batch of PDO from PP pyrolysis (at 390 min) exhibited the maximum yield of olefins. Certainly, the presence of PP in the feed increases the olefin concentration in PDOs. The paraffin concentration was increased with time while, the reverse trend followed for olefins. It was established in our previous study (Das and Tiwari, 2018) that the paraffinic content increases and olefinic content decrease with the increase of pyrolysis temperature. A similar observation was also made by Marcilla et al. (2009) by conducting pyrolysis of LDPE and HDPE under low-temperature range (360–385 °C) and reported that 1-olefin and n-paraffins are the major products. Table 5 also includes the data calculated using Eqs. (4)–(6) for H/C ratio, iso-paraffin index and RON values of PDOs. Higher values of H/C ratio (>1) indicate less emission of greenhouse gases if utilized as fuel alternatives (Sinag et al., 2006). PDOs from LDPE and HDPE have shown higher H/C ratio, which was apparently consistent with temperature. The isoparaffin index represents the proportion of branch paraffin to the normal paraffin (Sinag et al., 2006). Hence, elevated isoparaffin index implies high RON value. The isoparaffin index was found to be higher in case of PDO from PP and the values showed an increasing trend with temperature (reaction time) in
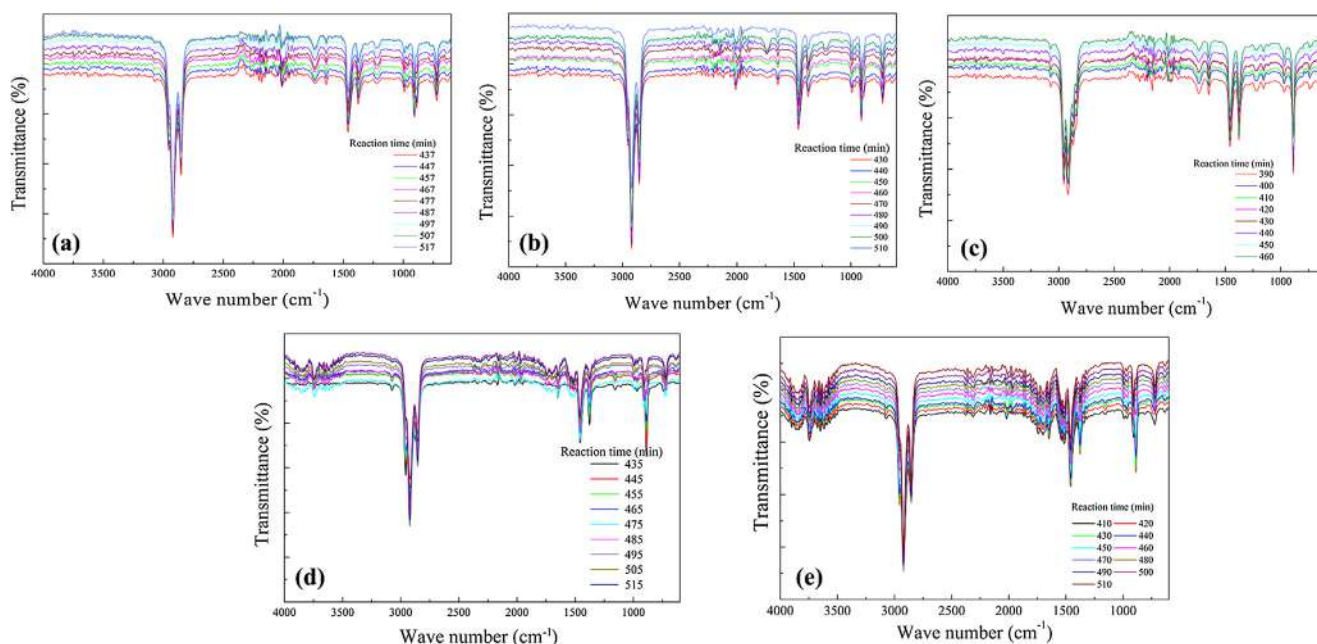

Fig. 4. FTIR-ATR spectra of PDOs obtained at different time intervals from (a) LDPE, (b) HDPE, (c) PP, (d) VMIX and (e) RMIX.

Table 5
Volume fractions of paraffin, olefin and aromatic, H/C, isoparaffin index and RON values of the PDOs.

Feed material	Pyrolysis time (min)	Paraffin (v/v%)	Olefin (v/v%)	Aromatic (v/v%)	H/C	Isoparaffin index	RON
LDPE	437	65.58	32.09	2.33	1.82	0.24	82.55
	447	60	37.3	2.7	1.8	0.25	82.74
	457	62.9	34.24	2.86	1.8	0.21	82.38
	467	65.89	31.83	2.28	1.82	0.19	82.2
	477	68	29.55	2.45	1.83	0.19	82.15
	487	69.46	27.69	2.85	1.82	0.16	81.97
	497	70.46	27.02	2.52	1.83	0.17	81.99
	507	68.36	28.69	2.95	1.82	0.18	82.08
	517	65.62	30.65	3.73	1.78	0.16	82.07
HDPE	430	49.49	47.69	2.82	1.75	0.22	82.5
	440	63.26	33.85	2.89	1.8	0.19	82.22
	450	64.5	32.65	2.85	1.8	0.19	82.21
	460	66.24	30.8	2.96	1.83	0.17	82.03
	470	67.27	29.33	3.4	1.81	0.16	81.96
	480	67.9	29.15	2.95	1.8	0.16	81.95
	490	66	31.37	2.63	1.77	0.16	81.9
	500	68.2	28.9	2.9	1.8	0.15	81.86
	510	72.13	25.03	2.84	1.83	0.19	80.42
PP	390	43.9	55.27	0.83	1.33	0.59	85.55
	400	55.51	43.1	1.38	1.64	0.98	89.07
	410	61.34	37.5	1.2	1.66	1.23	91.25
	420	59.67	38.67	1.37	1.62	1.32	92.1
	430	59.1	39.28	1.6	1.6	1.3	92.03
	440	59.04	39.6	1.36	1.61	1.42	93.02
	450	57.54	40.25	2.21	1.6	1.23	91.44
	460	62.08	35.93	1.98	1.65	1.34	92.36
VMIX	435	51.3	47.2	1.5	1.68	0.9	88.3
	445	56.88	41.52	1.6	1.7	0.75	87
	455	60.44	37.9	1.65	1.7	0.6	85.4
	465	60.59	37.33	2.08	1.7	0.61	86
	475	52.88	44.06	3.06	1.8	0.28	83.01
	485	61.87	35.2	2.92	1.76	0.22	82.5
	495	61.55	34.8	3.65	1.77	0.2	82.4
	505	61.86	34.1	4.05	1.8	0.2	82.33
	515	65.54	31.01	3.44	1.75	0.2	82.4
RMIX	410	63.15	33.85	3	1.76	0.49	84.86
	420	60.76	37.46	1.78	1.7	0.65	86.18
	430	58.9	39.5	1.62	1.7	0.7	86.6
	440	59.65	38.17	2.46	1.7	0.54	85.3
	450	61.61	36.04	1.52	1.76	0.27	82.94
	460	63.36	33.92	2.71	1.76	0.27	82.95
	470	64.71	32.84	3.6	1.76	0.2	82.38
	480	66.62	30.3	3.1	1.8	0.21	82.38
	490	66.49	30.12	3.42	1.8	0.2	82.34
	500	66.6	29.28	4.8	1.75	0.18	82.3
	510	65.58	28.93	7.39	1.78	0.19	82.3

case of PP, whereas in other feed conditions the isoparaffin index decreased with temperature. RON values appeared to be higher (Table 5) for the initial (low temperature) PDO samples from LDPE, HDPE, VMIX and RMIX. The PP polymer chain has a methyl group attached to every other carbon atom, which help in the formation of branched paraffins and olefins. According to Pinto et al. (1999) the presence of extra methyl group in the PP polymer chain stabilizes the intermediate radicals by forming a double bond between two carbon atoms. A qualitative explanation regarding the degradation mechanism of such polymers can be derived from various past studies (Marcilla et al., 2009; Simha et al., 1958; Singh and Sharma, 2008; Wall et al., 1954). It has been reported that under elevated temperature, such polyolefins breaks down into radicals by scission reaction. These radicals undergo stabilization (propagation) by intra or inter-molecular hydrogen transfer. Low temperature favours the intramolecular hydrogen transfer lead to the formation of olefins whereas increasing temperature shifts to intermolecular hydrogen transfer which results in more paraffins. The high concentration of olefins in the oil sample have huge industrial applications since, petrochemical olefins are initial feed-

stock for many industrial organic chemicals like vinyl acetate, acetaldehyde, and vinyl chloride and used as feedstock to many polymers. The unsaturated hydrocarbons (olefins) can undergo metathesis to cyclic and acyclic alkenes etc., which have greater industrial and commercial importance.

4.2.2. Simulated distillation (SimDist) analysis of PDO

The simulated distillation of the PDO samples was carried out and, the weight equivalent of peak areas were determined and converted into weight percent to establish the carbon number distribution. The distributed weight fractions were classified into light ($C_6 – C_{11}$), middle ($C_{12} – C_{20}$) and heavy ($C_{21} – C_{FBP}$) fractions, which resemble the conventional petroleum fractions.

The variations in the hydrocarbon fractions for each PDOs obtained at various time intervals during pyrolysis of each sample are shown in Figs. 5 and 6. Initial observations of Figs. 5 and 6 reflect high yield of light fractions during the initial stages of the plastic degradation, whereas the concentrations of middle and heavy fractions increased as the process progressed to a higher temperature. The PDOs from PP were comparatively lighter than
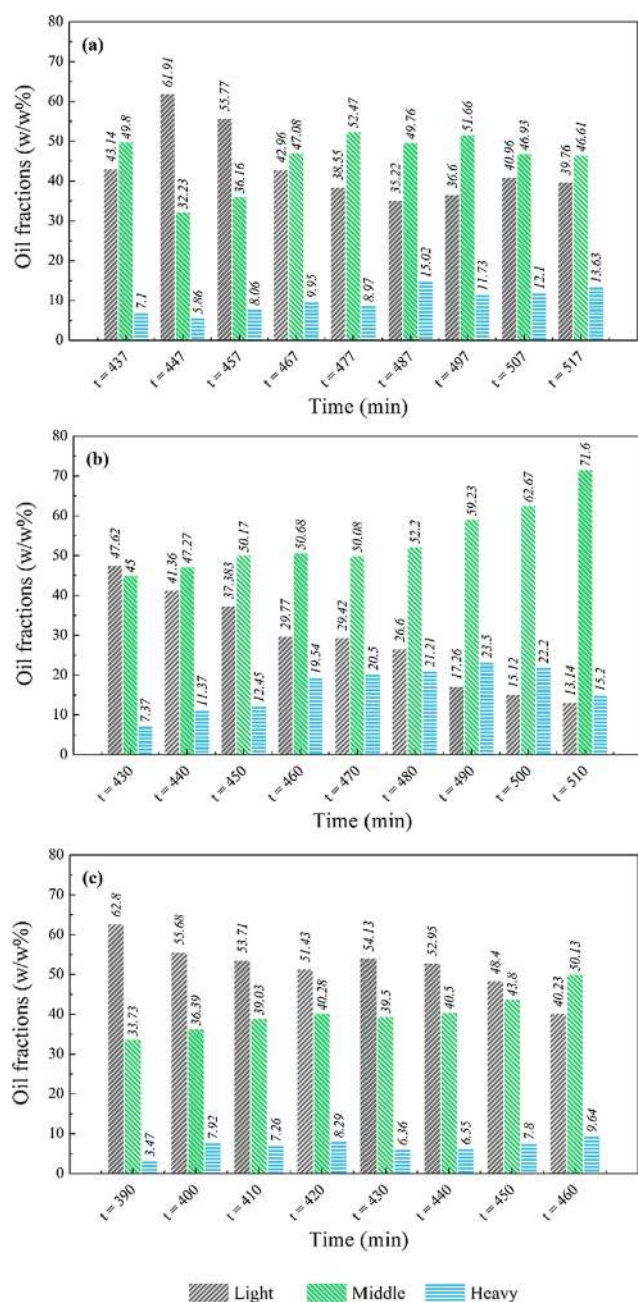
Fig. 5. Fractional distribution of PDOs obtained at different pyrolysis interval for (a) LDPE, (b) HDPE and (c) PP as feed.

the PDOs from other plastic feed as the concentration of the lighter fractions maintained a yield of more than 40% throughout the process with maximum value as 62.8% at 390 min (300 °C). Similarly, for the PDO from HDPE, the maximum concentration of middle fraction (71.6%) was obtained at 510 min. Similar distribution trends were noticed for LDPE (Fig. 5(a)) and for both the mixed plastic feeds (Fig. 6(a) and (b)). The highest concentrations of lighter fractions for VMIX and for RMIX were obtained at 445 min (305 °C) and 420 min (310 °C) respectively. The yields of the middle fractions for VMIX and RMIX were found minimum (around 30%) at 445 min (310 °C) and 430 min (325 °C) respectively. The ultimate aim to do the non-isothermal slow pyrolysis is establishing the pyrolysis condition that can enhance the possibility of producing a particular value-added product. To understand further, boiling point distribution (carbon number) curves with cumulative

yields for the PDOs obtained from RMIX are shown in Fig. 7. It was observed that around 85% PDOs obtained before 450 min (360 °C) have distillation range under 350 °C and belongs to a carbon number distribution range of $C_6 – C_{20}$. The fractional ($C_6 – C_{20}$) yield decreased to 70% as the pyrolysis temperature increased to 400 °C (510 min). Similar boiling point (carbon number) distribution profiles for the other feeds are shown in Fig. 4S. A difference in the carbon number distribution with temperature occurs as the reaction progressed. Under the influence of heat, the polymer chain of polyolefins breaks (end chain or random chain scission) at weak links (sp^3 bond) and forms radicals. Most of the scission reactions in polymer degradation occurred at β position of the polymer chain. The end chain β-scission requires less energy than random chain β scission. Both random and end chain β scission reactions are responsible for the formation of the gaseous fraction and the light and middle fractions of the liquid. Low temperature favours the production of lighter fractions of the liquid. At high temperature pyrolysis, the liquid fraction undergoes secondary reactions to produce more uncondensed hydrocarbon gases. Table 6 summarizes the results obtained in the present study along with the data reported in the literature. The distribution of product compositions (paraffins/olefins) with temperature is evident in most of the findings reported by others (Marcilla et al., 2009; Williams and Slaney, 2007; Zanella et al., 2013). A common conclusion that can be drawn is that lowering the heating rate for the pyrolysis process of packaging plastics, a better control over the process to target a certain value-added product like light/middle distillate of petroleum can be achieved.

4.2.3. Pyrolysis gas analysis

The compositions of the evolved gases during plastic pyrolysis with temperature rise is a required for sustainable implementation of the process. The evolve gases from the pyrolysis of plastics (polyolefins) contain hydrocarbon gases like methane, ethane, ethylene, propane, propylene, propadiene, acetylene, n-butane, trans-2-butene, 1-butene, isobutylene, cis-2-butene, isopentane, n-pentane, methyl acetylene, including a trace amount of inorganic gases like H_2, CO_2 and CO etc. Presence of these hydrocarbon components in the off-gases exhibits their potential use as fuel gas due to high calorific value (Das and Tiwari, 2018). The variations in the concentration (v/v %, N_2 free basis) of major gaseous components present in the gas samples collected at different time are shown in Fig. 8 for LDPE, HDPE and PP and in Fig. 9 for VMIX and RMIX. The concentrations of the hydrocarbon gases varied as the pyrolysis reaction proceeds. The yield of individual component achieved a maximum value at a particular temperature and then decreased. This is because of the fact that the gaseous product having high molecular weight components produced at higher pyrolysis temperature undergoes condensation. However, sharp decrease in the gas yield at the end of the process may be attributed to the lack of any volatile substance in the reactor. The concentration of propylene was found dominating (∼22–25 v/v%) in the gaseous product for all the feed conditions and throughout the gas generation period. Other gases like ethane, propane, butane and ethylene were found in significant amount in case of LDPE and HDPE as feed [Fig. 8(a) and (b)], whereas isobutylene and pentane concentrations were higher in case of PP [Fig. 8(c)]. Similar gas evolution pattern was also observed for VMIX (Fig. 9). However, RMIX feed produced relatively more methane at various stages of the process [Fig. 9(b)]. The evolution of methane, ethane, ethylene, propane, and n-butane was also reported by Singh and Ruj (2016) from the pyrolysis of municipal plastic waste at isothermal condition (450–600 °C). Marcilla et al. (2009) observed a higher yield of C_3 components (propane and propylene) as compared to other hydrocarbon gases.
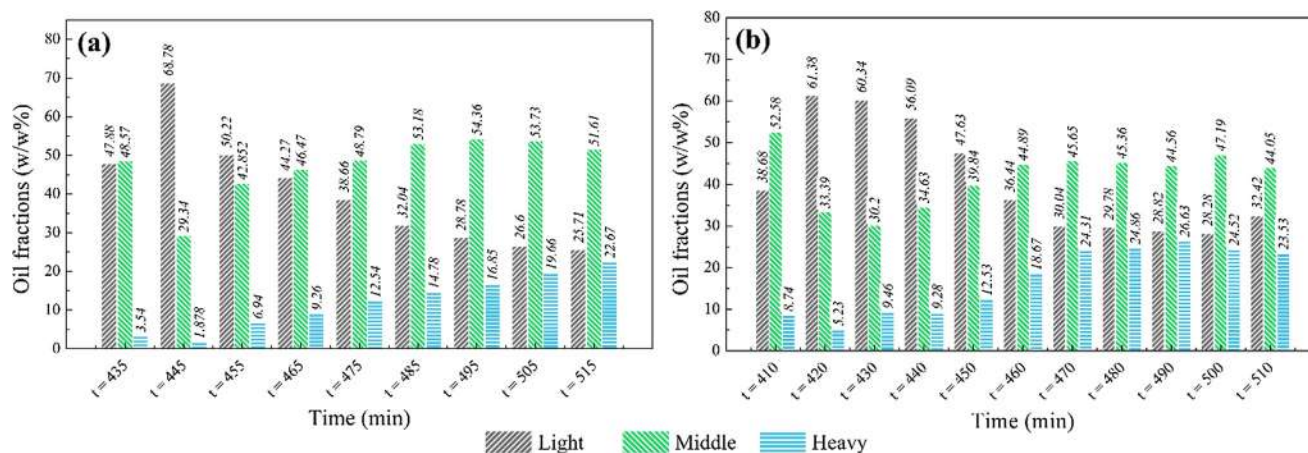
Fig. 6. Fractional distribution of PDOs obtained at different pyrolysis interval for (a) VMIX and (b) RMIX.
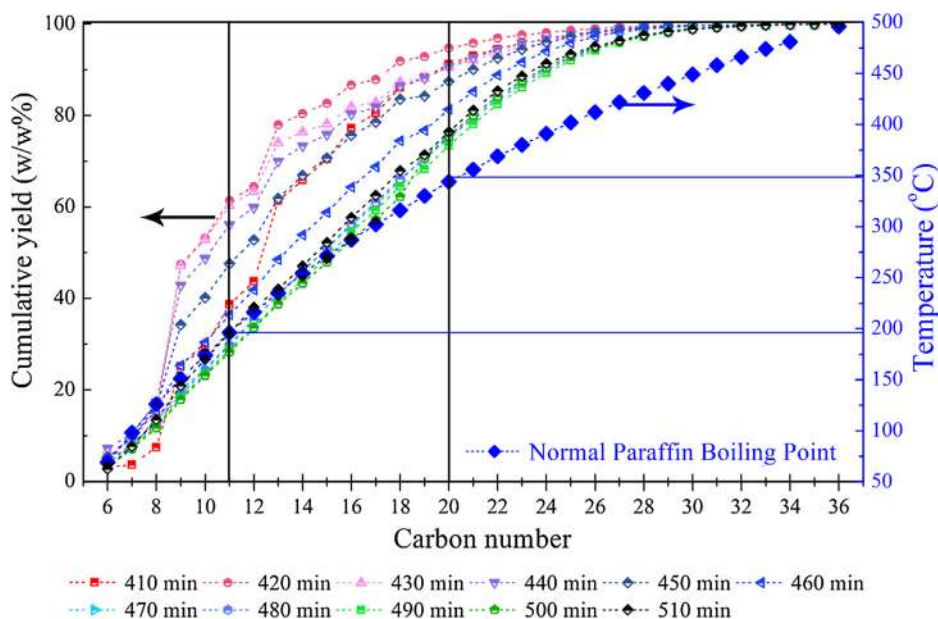

Fig. 7. Cumulative yield (w/w%) of hydrocarbons with respect to carbon number and the boiling range of n-paraffins and for PDO obtained at various time interval of non-isothermal pyrolysis of RMIX sample.

Table 6
Comparison of current study with other works considering slow pyrolysis of packaging plastics.

References	Material	Reactor type	Pyrolysis condition	Liquid yield/quality
Williams and Slaney (2007)	Simulated plastic mixture with HDPE as major component	Pressurised batch autoclave	β = 5 °C·min^{-1}; T_f = 500 °C; t_h = 1 h; under N$_2$ and H$_2$ gas; P_0 = 0.2 MPa	48.7% (N$_2$); Paraffin concentration is more
Marcilla et al. (2009)	LDPE; HDPE (virgin powder form)	Batch reactor	β = 5 °C·min^{-1}; T_f = 550 °C; N$_2$ flow rate = 150 ml·min^{-1};	Paraffin and olefins are major component but % yield of most components pass through a maximum as temperature increases
Onwudili et al. (2009)	LDPE; PS	Pressurised batch autoclave	β = 10 °C·min^{-1}; T_f = 350–500 °C; t_h = 1 h	At 425 °C; 44 wt% paraffin and 11.6 wt% olefins
Grieco and Baldi (2012)	LDPE; beech sawdust; paper	Stainless steel capsule in oven	β = 1 °C·min^{-1} and 0.1 °C/min	86.2% tar at 1 °C/min and 90.9% tar at 0.1 °C·min^{-1} (from pure LDPE)
Zanella et al. (2013)	PP; coffee	Fixed bed reactor	β = 5 °C·min^{-1}; T_f = 360–480 °C; t_h = 3 h (inert gas: Ar/N$_2$)	Heavy fraction increases with the increase of temperature
Current study	LDPE; HDPE; PP and their mixture (virgin/real waste)	Semi-batch pyrolysis reactor	β = 1 °C·min^{-1}; T_f = 400 °C (reactor); t_h = 1 h;	Liquid yield at low temperatures have short chain hydrocarbons with high octane number and RON

β = heating rate; T_f = final temperature; t_h = isothermal holding time; P_0 = initial pressure and PS = polystyrene.
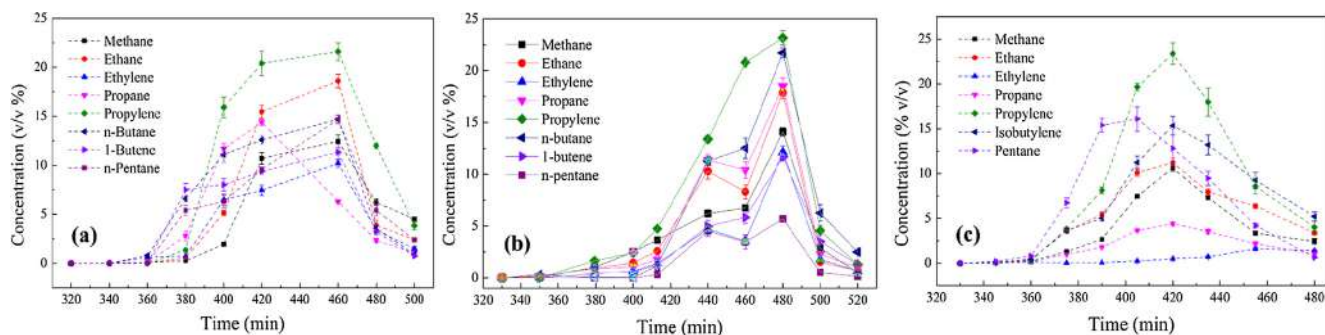
Fig. 8. Distribution of hydrocarbon gases over various interval of slow pyrolysis for (a) LDPE; (b) HDPE and (c) PP.
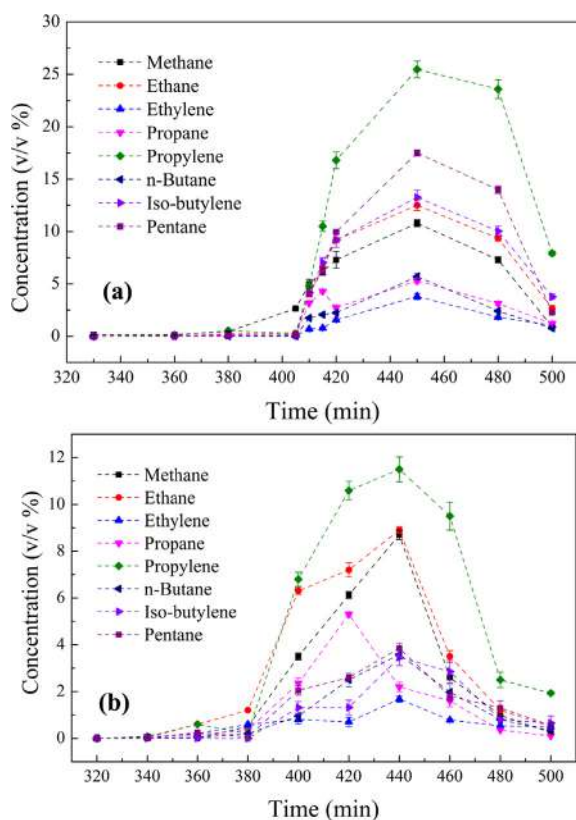

Fig. 9. Distribution of hydrocarbon gases over various interval of slow pyrolysis for (a) VMIX and (b) RMIX.

5. Conclusion

Non-isothermal slow pyrolysis of polyolefins (LDPE, HDPE and PP) provides a detail understanding of the influence of reaction temperature on the product distribution. The utilization of slow pyrolysis as an alternative approach to produce targeted value added product (gasoline/diesel) from plastic waste is significant considering the plastic disposal and management issues. NMR analysis of the PDO obtained from PP has shown encouraging prospects of producing gasoline blend components with a very high RON value (~92). High values of H/C ratio of the PDOs ensures clean burning if use as liquid fuel. PDO samples obtained at low temperatures have higher percentage of lighter fractions ($C_6 – C_{11}$). The evolution of hydrocarbon gas also varies as the process progresses, due to the effect of temperature on gas formation. The overall gas yield ($<C_6$) decreases with the initiation of gas condensation. Propylene concentration was found to be higher compared to other gases. The gas evolved during pyrolysis will play a significant role in the implementation of the process as most of these gases have high calorific value and can be exploited as a fuel source for the process. However, more in-depth research is necessary in terms of large-scale implementation. This study provides valuable insights, which may help designing and optimizing pyrolysis process plant to convert packaging plastic waste into valuable fuel.

References

Aguado, J., Serrano, D.P., Escola, J.M., Garagorri, E., 2002a. Catalytic conversion of low-density polyethylene using a continuous screw kiln reactor. Catal. Today 75, 257–262.

Aguado, R., Olazar, M., San José, M.J., Gaisán, B., Bilbao, J., 2002b. Wax formation in the pyrolysis of polyolefins in a conical spouted bed reactor. Energy Fuels 16, 1429–1437.

Albahri, T.A., 2003. Structural group contribution method for predicting the octane number of pure hydrocarbon liquids. Indus. Eng. Chem. Res. 42, 657–662.

Chattopadhyay, J., Pathak, T.S., Srivastava, R., Singh, A.C., 2016. Catalytic co-pyrolysis of paper biomass and plastic mixtures (HDPE (high density polyethylene), PP (polypropylene) and PET (polyethylene terephthalate)) and product analysis. Energy 103, 513–521.

Chaukura, N., Gwenzi, W., Bunhu, T., Ruziwa, D.T., Pumure, I., 2016. Potential uses and value-added products derived from waste polystyrene in developing countries: a review. Resour. Conserv. Recy 107, 157–165.

Costa, P., Pinto, F., Ramos, A.M., Gulyurtlu, I., Cabrita, I., Bernardo, M.S., 2010. Study of the pyrolysis kinetics of a mixture of polyethylene, polypropylene, and polystyrene. Energy Fuels 24, 6239–6247.

Das, P., Tiwari, P., 2017. Thermal degradation kinetics of plastics and model selection. Thermochim. Acta 654, 191–202.

Das, P., Tiwari, P., 2018. Valorization of packaging plastic waste by slow pyrolysis. Resour. Conserv. Recy 128, 69–77.

Elordi, G., Olazar, M., Lopez, G., Amutio, M., Artetxe, M., Aguado, R., Bilbao, J., 2009. Catalytic pyrolysis of HDPE in continuous mode over zeolite catalysts in a conical spouted bed reactor. J. Anal. Appl. Pyrol. 85, 345–351.

Geyer, R., Jambeck, J.R., Law, K.L., 2017. Production, use, and fate of all plastics ever made. Sci. Adv., vol. 3.

Grieco, E.M., Baldi, G., 2012. Pyrolysis of polyethylene mixed with paper and wood: Interaction effects on tar, char and gas yields. Waste Manage. 32, 833–839.

Jambeck, J.R., Geyer, R., Wilcox, C., Siegler, T.R., Perryman, M., Andrady, A., Narayan, R., Law, K.L., 2015. Plastic waste inputs from land into the ocean. Science 347, 768.

Joo, H.S., Guin, J.A., 1998. Continuous upgrading of a plastics pyrolysis liquid to an environmentally favorable gasoline range product. Fuel Process. Technol. 57, 25–40.

Kaminsky, W., Predel, M., Sadiki, A., 2004. Feedstock recycling of polymers by pyrolysis in a fluidised bed. Polym. Degrad. Stab. 85, 1045–1050.

Kaminsky, W., Schlesselmann, B., Simon, C., 1995. Olefins from polyolefins and mixed plastic by pyrolysis. J. Anal. Appl. Pyrol. 32, 19–27.

Kamyotra, J.S., Sinha, D., 2016. CPCB Bulletin. Central Pollution Control Board, Delhi, pp. 20–21.

Kumar, S., Panda, A.K., Singh, R.K., 2011. A review on tertiary recycling of high-density polyethylene to fuel. Resour. Conserv. Recy 55, 893–910.

Lopez-Urionabarrenechea, A., de Marco, I., Caballero, B.M., Laresgoiti, M.F., Adrados, A., 2012. Catalytic stepwise pyrolysis of packaging plastic waste. J. Anal. Appl. Pyrol. 96, 54–62.

Lopez, G., Artetxe, M., Amutio, M., Bilbao, J., Olazar, M., 2017. Thermochemical routes for the valorization of waste polyolefinic plastics to produce fuels and chemicals. A review. Renew. Sustain. Energy Rev. 73, 346–368.

Ludlow-Palafox, C., Chase, H.A., 2001. Microwave-induced pyrolysis of plastic wastes. Indus. Eng. Chem. Res. 40, 4749–4756.

Marcilla, A., Beltrán, M.I., Navarro, R., 2009. Evolution of products during the degradation of polyethylene in a batch reactor. J. Anal. Appl. Pyrol. 86, 14–21.

Miandad, R., Barakat, M.A., Aburiazaiza, A.S., Rehan, M., Nizami, A.S., 2016. Catalytic pyrolysis of plastic waste: a review. Process Saf. Environ. Prot. 102, 822–838.

Myers, M.E., Stollstelmer, J., Wims, A.M., 1975a. Determination of gasoline octane numbers from chemical composition. Anal. Chem. 47, 2301–2304.

Myers, M.E., Stollstelmer, J., Wims, A.M., 1975b. Determination of hydrocarbon-type distribution and hydrogen/carbon ratio of gasolines by nuclear magnetic resonance. Anal. Chem. 47, 2010–2015.

Onwudili, J.A., Insura, N., Williams, P.T., 2009. Composition of products from the pyrolysis of polyethylene and polystyrene in a closed batch reactor: effects of temperature and residence time. J. Anal. Appl. Pyrol. 86, 293–303.

Pinto, F., Costa, P., Gulyurtlu, I., Cabrita, I., 1999. Pyrolysis of plastic wastes. 1. Effect of plastic waste composition on product yield. J. Anal. Appl. Pyrol. 51, 39–55.

Serrano, D.P., Aguado, J., Escola, J.M., Garagorri, E., 2003. Performance of a continuous screw kiln reactor for the thermal and catalytic conversion of polyethylene–lubricating oil base mixtures. Appl. Catal. B 44, 95–105.

Siddiqui, M.N., Redhwi, H.H., 2009. Pyrolysis of mixed plastics for the recovery of useful products. Fuel Process. Technol. 90, 545–552.

Simha, R., Wall, L.A., Bram, J., 1958. High-speed computations in the kinetics of free-radical degradation. I. Random initiation. J. Chem. Phys. 29, 894–904.

Sinag, A., Sungur, M., Gullu, M., Canel, M., 2006. Characterization of the liquid phase obtained by copyrolysis of mustafa kemal pasüa (M.K.P.) lignite (Turkey) with low density polyethylene. Energy Fuels 20, 2093–2098.

Singh, B., Sharma, N., 2008. Mechanistic implications of plastic degradation. Polym. Degrad. Stab. 93, 561–584.

Singh, R.K., Ruj, B., 2016. Time and temperature depended fuel gas generation from pyrolysis of real world municipal plastic waste. Fuel 174, 164–171.

Undri, A., Meini, S., Rosi, L., Frediani, M., Frediani, P., 2013. Microwave pyrolysis of polymeric materials: waste tires treatment and characterization of the value-added products. J. Anal. Appl. Pyrol. 103, 149–158.

Wall, L.A., Madorsky, S.L., Brown, D.W., Straus, S., Simha, R., 1954. The depolymerization of polymethylene and polyethylene. J. Am. Chem. Soc. 76, 3430–3437.

Williams, E.A., Williams, P.T., 1997a. Analysis of products derived from the fast pyrolysis. J. Anal. Appl. Pyrol. 40–41, 347–363.

Williams, E.A., Williams, P.T., 1997b. The pyrolysis of individual plastics and a plastic mixture in a fixed bed reactor. J. Chem. Technol. Biotechnol. 70, 9–20.

Williams, P.T., Slaney, E., 2007. Analysis of products from the pyrolysis and liquefaction of single plastics and waste plastic mixtures. Resour. Conserv. Recy 51, 754–769.

Williams, P.T., Williams, E.A., 1999. Interaction of plastics in mixed-plastics pyrolysis. Energy Fuels 13, 188–196.

Wong, H., Broadbelt, L.J., 2001. Tertiary resource recovery from waste polymers via pyrolysis: neat and binary mixture reactions of polypropylene and polystyrene. Indus. Eng. Chem. Res. 40, 4716–4723.

Xue, Y., Kelkar, A., Bai, X., 2016. Catalytic co-pyrolysis of biomass and polyethylene in a tandem micropyrolyzer. Fuel 166, 227–236.

Zanella, E., Della Zassa, M., Navarini, L., Canu, P., 2013. Low-temperature co-pyrolysis of polypropylene and coffee wastes to fuels. Energy Fuels 27, 1357–1364.